

# Dissipative Structures in 1D and 2D Chemically Reacting Systems

P. Nandapurkar and V. Hlavacek

Department of Chemical Engineering, State University of New York at Buffalo,  
Clifford C. Furnas Hall, Buffalo, New York, USA

Z. Naturforsch. **38a**, 963–973 (1983); received April 14, 1983

A transient analysis of the 1D and 2D reaction-diffusion equations associated with the model reaction of Prigogine and Lefever (Brusselator model), including diffusion of the initial (substrate) component, has been performed. For low system lengths and for fixed boundary conditions, the steady state low amplitude solutions are unstable. For zero flux boundary conditions a multiplicity of symmetric solutions with the same wave number may exist, the majority of them being unstable. The diffusion of initial components induce relaxation oscillations in space both for fixed as well as zero flux boundary conditions. The amplitude of the oscillation increases as the diffusion coefficient of the initial component decreases. For conditions of relaxation oscillations the spatial profiles result in single or multiple propagating fronts.

High system lengths (or low diffusion coefficient of intermediate components), for both zero flux and periodic boundary conditions, may give rise to a multipeak incoherent wave pattern. For periodic boundary conditions a multiplicity of waves has been observed. Numerical simulation of the 2D-spatial structures reveal certain similarities between the 1D and 2D cases.

## 1. Introduction

It is widely known that the interaction of reaction and diffusion in an open system operating far from the thermodynamic equilibrium gives rise to many interesting phenomena such as multiple spatially ordered steady states, spatially homogeneous periodic solutions, nonhomogeneous periodic solutions, travelling waves and fronts, shock structures, etc. [1–3]. Prigogine and Nicolis [4] have termed these structures arising in the reaction-diffusion systems as dissipative structures. Since the classical paper by Prigogine and Nicolis in 1967 [5], the volume of literature in this field has been growing steadily. The reaction-diffusion equations coupled with appropriate kinetic expressions have been shown to serve as simple models of a number of biological phenomena and may also explain similar phenomena in many other fields.

The occurrence of multiple stable solutions for the Brusselator chemical network has been analytically predicted (via the bifurcation theory) and confirmed numerically by Herschkowitz-Kaufman [1] and Nicolis et al. [4]. For this model they have reported multiple stable symmetric and asymmetric steady state solutions, homogeneous periodic solu-

tions and travelling waves in one dimension while for a two dimensional geometry (circle) they have obtained rotating waves and nonhomogeneous periodic solutions. Kubicek et al. [6] have numerically constructed a typical bifurcation diagram for this network by employing a continuation algorithm. In their study the primary bifurcation points were located analytically while the space profiles were computed numerically. The calculated steady state profiles were tested for stability and asymptotic behavior. The Brusselator chemical network has been subjected to many theoretical investigations since it exhibits many interesting phenomena and is easy to analyse because of a single homogeneous (thermodynamic) solution. In the majority of previous studies the initial components *A* and *B* are assumed to be maintained uniform throughout the system by some external mechanism. A realistic description, however, requires the inclusion of diffusion of these components. In this paper, therefore, we consider a modified Brusselator model which includes the diffusion of initial components. Here we are going to investigate the stability of computed steady state solutions via transient analysis, consider the effect of diffusion of initial components on the periodicity of solutions, study the equivalence between one and two dimensional geometries and report on some numerically observed periodic solutions in one and two space dimensions.

Reprint requests to Prof. V. Hlavacek, Department of Chemical Engineering, State University of New York at Buffalo, Clifford C. Furnas Hall, Buffalo, New York 14260, USA.

0340-4811 / 83 / 0900-0963 \$ 01.3 0/0. – Please order a reprint rather than making your own copy.



Dieses Werk wurde im Jahr 2013 vom Verlag Zeitschrift für Naturforschung in Zusammenarbeit mit der Max-Planck-Gesellschaft zur Förderung der Wissenschaften e.V. digitalisiert und unter folgender Lizenz veröffentlicht: Creative Commons Namensnennung-Keine Bearbeitung 3.0 Deutschland Lizenz.

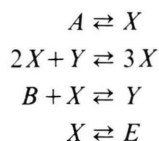
Zum 01.01.2015 ist eine Anpassung der Lizenzbedingungen (Entfall der Creative Commons Lizenzbedingung „Keine Bearbeitung“) beabsichtigt, um eine Nachnutzung auch im Rahmen zukünftiger wissenschaftlicher Nutzungsformen zu ermöglichen.

This work has been digitalized and published in 2013 by Verlag Zeitschrift für Naturforschung in cooperation with the Max Planck Society for the Advancement of Science under a Creative Commons Attribution-NoDerivs 3.0 Germany License.

On 01.01.2015 it is planned to change the License Conditions (the removal of the Creative Commons License condition “no derivative works”). This is to allow reuse in the area of future scientific usage.

## 2. Brusselator Model and the Reaction Diffusion Equations

The "Brusselator" model, originally proposed by Prigogine and Lefever [7] corresponds to the following trimolecular scheme.



As mentioned earlier, in the majority of previous studies the concentrations of the initial components  $A$  and  $B$  have been assumed to be maintained uniform (e.g. large excess of  $A$  and  $B$  or infinite diffusion coefficients,  $D_A \rightarrow D_B \rightarrow \infty$ ). In the present investigation, we include the diffusion of component  $A$  but treat  $B$  to be uniform. After neglecting all the reverse reactions and setting the rate constants to unity, following reaction-diffusion equations are obtained:

$$\partial A / \partial t = -A + D_A \nabla^2 A, \quad (1)$$

$$\partial X / \partial t = A + X^2 Y - (B + 1) X + D_x \nabla^2 X, \quad (2)$$

$$\partial Y / \partial t = B X - X^2 Y + D_y \nabla^2 Y. \quad (3)$$

In these equations  $\nabla$  is the Laplacian operator while  $D_x$  and  $D_y$  are the diffusion coefficients for  $X$  and  $Y$ . For a one dimensional model  $\nabla$  is given by

$$\nabla^2 = \partial^2 / \partial z^2 \quad (4)$$

while for a two dimensional cartesian coordinate system

$$\nabla^2 = \frac{\partial^2}{\partial x^2} + \frac{\partial^2}{\partial y^2}. \quad (5)$$

The following boundary conditions are considered:

### (a) Fixed boundary conditions

For a one dimensional system:

$$z = 0, L; t > 0: X = X_0, Y = Y_0. \quad (6)$$

For a two-dimensional geometry:

$$x = 0, 1; y = 0, 1; t > 0: X = X_0, Y = Y_0. \quad (7)$$

### (b) Zero flux boundary conditions

In one dimension:

$$z = 0, L; t > 0: \partial X / \partial z = \partial Y / \partial z = 0. \quad (8)$$

For a two dimensional case:

$$x = 0, 1, \quad \partial X / \partial x = \partial Y / \partial x = 0, \quad (9)$$

$$y = 0, 1, \quad \partial X / \partial y = \partial Y / \partial y = 0. \quad (10)$$

### (c) Periodic boundary conditions

$$X(0) = X(z), \quad \frac{\partial X}{\partial z}(0) = \frac{\partial X}{\partial z}(z), \quad (11)$$

$$Y(0) = Y(z), \quad \frac{\partial Y}{\partial z}(0) = \frac{\partial Y}{\partial z}(z). \quad (12)$$

For these boundary conditions we have considered the one dimensional system only. Further, as is apparent from the physics of the problem this type of boundary condition does not allow for inflow and outflow and hence we cannot consider the diffusion of component  $A$ .

## 3. Numerical Method of Solution

Equations (1) to (3) represent a set of coupled non-linear parabolic partial differential equations. However (1) is separable form (2) and (3) and can be solved independently to obtain the following steady state solution in one dimension

$$A(z) = A_0 \frac{\cosh \left[ \frac{1}{\sqrt{D_A}} (z - L/2) \right]}{\cosh \left[ \frac{L}{2\sqrt{D_A}} \right]}. \quad (13)$$

Equations (2) and (3), however, are coupled by the nonlinear source term and this necessitates its solution numerically. In our numerical calculations, we have used a Störmer-Numerov finite difference approximation for the space derivative. This method has  $(h^4, k^2)$  accuracy but needs only 3 mesh points in space. The details of this techniques with applications has been described elsewhere [8].

Following extrapolation formula has been used to evaluate the source term at time grid  $j + \frac{1}{2}$

$$\bar{\theta}^{j+1/2} = 1.5 \theta^j - 0.5 \theta^{j-1}. \quad (14)$$

The method of solution also features automatic time step adjustment which is done on the basis of error between the predicted and the extrapolated values for the source term. For the case of periodic boundary conditions the finite difference scheme introduces an off diagonal element in the tridiagonal

nal structure and the fast solution method of Evans [9] has been used.

For two dimensional problems the conventional 5-point difference scheme requires solution of a banded matrix structure which is expensive. We have therefore used the ADI (Alternate direction implicit) method to calculate the space profiles in two dimensions. All the reported calculations have been performed on CDC CYBER 173 machine.

#### 4. Results and Discussions

The following parameter values have been used in numerical calculations.

(1) Steady-state solutions:  $A = 2.0$ ,  $B = 4.6$ ,  $D_x = 0.0016$  and  $D_y = 0.008$ .  $D_A = 0.1$  for fixed boundary conditions and equals 0.02 for zero flux boundary conditions.  $L$  is reported with each figure.

(2) Periodic solutions:  $A = 2.0$ ,  $D_x = 0.008$  and  $D_y = 0.004$ . The variation in  $L$ ,  $B$  and  $D_A$  is reported along with each figure. Values of parameters other than presented above are indicated in the description of figures.

(a) Stability of steady state solutions: The bifurcation diagrams which indicate the number and the nature of solutions of a reaction-diffusion system are usually constructed from the steady state analysis of Eqs. (1) to (3). A typical bifurcation diagram for the present system has been constructed by

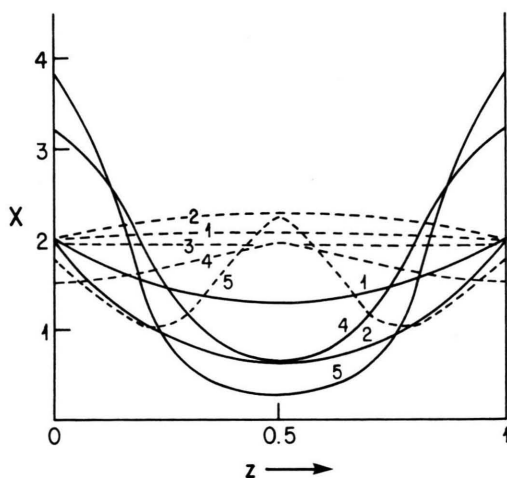


Fig. 1. Spatial profiles for  $X$ . - - - - Steady state solution; ——— transient simulation.

Profile	1	2	3	4	5
Length	0.1	0.17	0.1	0.2	0.3

Hlavacek et al. [10]. The solutions obtained from such steady state analysis need not be stable and, therefore, their stability must be investigated. For this purpose we take these steady state solutions, perturb them by about 1% and study the transient behavior of the system. The solution obtained at  $t \rightarrow \infty$  is considered as the asymptotic solution. Some of the results obtained are shown in Figure 1. The dashed lines represent the solutions calculated from the steady-state analysis while the solid lines represent the corresponding stable steady state solutions obtained at  $t \rightarrow \infty$ . It can be observed from this figure that unstable symmetric solutions (curves 1, 2, and 4) give rise to stable symmetric solutions with a phase shift. The unstable steady state solutions (dashed lines) 1 and 2, form a part of an isolated branch on the bifurcation diagram (Fig. 4 in [10]) and are very close to the thermodynamic solution for the fixed boundary conditions. Thus the solutions with low amplitude (deviations from the thermodynamic branch) seem to be unstable and the evolution process under these conditions will attract the trajectory to stable high amplitude solutions. We have further analyzed the stability of these solutions — by the one point collocation method [11]. The advantage of this method is it converts a system of partial differential equations (hereafter called as PDE) to ordinary differential equations (referred to as ODE) which are easier to deal with than the original PDE. In this method, we place one internal point at the center of the system and write down the finite difference equations for this point. Since the boundary points are fixed, this results in a single differential equation, which can be analyzed easily to obtain approximate results. On using the Störmer-Numov finite difference approximation, the differential equation describing the centre point can be written as:

$$10 \frac{dX_m}{dt} = 12 \frac{D_x}{h^2} (X_b - 2X_m + X_b) + 10 (A_m + X_m^2 Y_m - (B + 1) X_m), \quad (15)$$

where the subscript  $m$  denotes the value of the variable at the center point while subscript  $b$  denotes the value at the boundary. Similar equation can be obtained for  $Y_m$ . Thus, we now have an initial value problem to integrate. By setting  $dX_m/dt$  and  $dY_m/dt = 0$ , one can obtain the steady state values for the center point by solving the resulting nonlinear alge-

Table 1. Comparison of exact and approximate values.

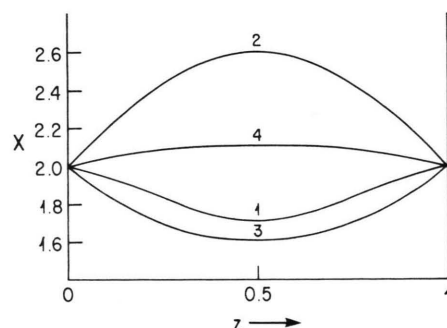
	Profile 1		Profile 2	
	$X$	$\bar{X}$	$X$	$\bar{X}$
$L = 0.10$	6.00	5.56	1.20	1.34
$L = 0.17$	0.60	0.78	3.00	2.79

braic equations. On using this approach we obtained the following approximate values for the center point which are given in Table 1. In this table  $X$  indicates the value obtained by solving the full PDE's while  $\bar{X}$  denotes the value obtained from the one point collocation. The agreement is quite satisfactory and one can use this information as a first approximation. It was noticed earlier that low amplitude solutions are unstable for fixed boundary conditions. However, they have been found to be stable for zero flux boundary conditions (curve 3). For the zero flux boundary conditions ( $L = 0.2$ ) Hlavacek et al. (10) have reported 7 steady state profiles. Three of these profiles are symmetric with 2 solutions having the same wave number but different amplitudes. One of these solutions is unstable (profile 4) and the stable solution is observed to be a symmetric solution with a phase shift. It, therefore, appears that steady solutions with the same wave number but different amplitudes may not be stable at low system lengths. Profile 5, which represents a high wave number (wave number equal to 3) solution for the zero flux boundary conditions is also unstable and the steady solution ( $t \rightarrow \infty$ ) has been found to have a wave number of one.

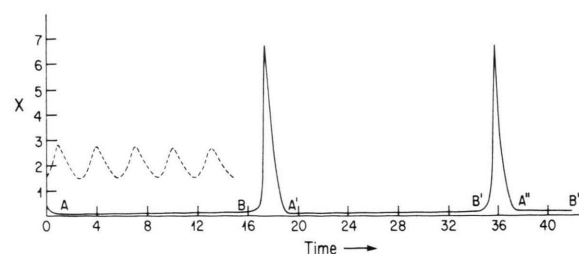
#### b) Periodic Solutions in One Dimension

Depending upon the values of the kinetic and diffusion constants and the system size  $L$ , the solution bifurcating from the thermodynamic branch could either be a stable steady state or a periodic solution. Such periodic solutions may give rise to concentration waves. Pismen (12) in describing the bifurcating waves has proposed that in a one dimensional system, depending upon initial conditions, the periodic solution may either be a propagating wave (in infinite system) or a standing wave (for a finite system), an ordered combination of standing waves or an incoherent pattern. Nicolis et al. [3] have analytically predicted and numerically observed the existence of standing and travelling waves for the Brusselator model.

These general results obtained from the bifurcation theory may not be applicable when diffusion of initial components is also considered. Since trivial solutions ( $X_0 = A$  and  $Y_0 = B/A$ ) for the present case do not exist, it also excludes the possibility of homogeneous periodic solutions. In such a case, the first bifurcating solution, therefore, is space dependent. This solution is symmetrical and represents a standing wave. For the chosen parameters ( $A = 2.0$ ,  $B = 5.8$ ,  $D_x = 0.008$ ) the solution at low bifurcation lengths ( $L$  up to 0.6) was always symmetrical for fixed boundary conditions. Various initial non-uniform profiles were tested to see whether asymmetric solutions exist. However, in each case, after an initial transient period the solution always evolved to a symmetric standing wave. A typical solution is shown in Figure 2. An interesting observation was made while studying the effect of diffusion of component  $A$  on periodic solutions. It was observed that the diffusion of component  $A$  alters the period as well as the nature of oscillations. A plot of oscillations at the center point of the system is shown in Figure 3. For the sake of comparison, the case with

Fig. 2. Periodic solution profile for  $X$ .  $L = 0.4$ ,  $B = 5.4$ ,  $D_A = 0.1$ .

Profile	1	2	3	4
Time	11.80	12.72	13.92	15.15

Fig. 3. Oscillations of the centre point.  $L = 0.6$ ,  $B = 5.4$ , ---  $D_A \rightarrow \infty$ , —  $D_A = 0.02$ .



constant  $A$  ( $D_A \rightarrow \infty$ ) is also shown on the same figure. It is observed from this figure that when  $D_A \rightarrow \infty$ , the oscillations are fairly regular. However, with the diffusion of component  $A$  these regular oscillations change to a period of fairly low and uniform concentration of  $X$  followed by a steep spike. The period elapsed between two successive spikes is also the same. This effect seems to be quite similar to the concentration oscillations observed for the Belousov-Zhabotinsky reaction (13). It, therefore, appears that the nonuniform distribution of component  $A$  gives rise to multiple time scales in the system. During the period  $A - B$  or  $A' - B'$ , the rate of change of the component  $X$  is very low and the system appears to be almost quiescent. This period of uniformity is followed by a period of rapid transformations which involves steep time gradients. Such type of phenomena has been termed as relaxation oscillations. Herschkowitz-Kaufman and Nicolis (14) have also reported relaxation oscillations for this model but they have analyzed only fixed boundary conditions. The transient space profiles during the period  $B' - A''$  are shown in Fig. 4(a) while Fig. 4(b) depicts the transient profiles in the region  $A' - B'$ . These figures reveal that during the short time scale propagating fronts are observed which move from the boundary towards the centre, collide and ultimately change to a standing wave pattern, which is carried into the quiescent region  $A'' - B''$  as shown in Figure 4(b). In order to explain the existence of the propagating fronts in the short time interval, we can make use of the theory of propagation of fronts and discontinuity by Ortoleva and Ross (15). According to this theory propagating fronts are observed for systems with kinetics on multiple time scale and possessing multiple homogeneous stationary states. Since these phenomena are observed with nonuniform distribution of component  $A$ , it is suspected that diffusion of  $A$  may cause the introduction of multiple pseudo stationary states (although for the Brusselator model with constant  $A$  only one stationary homogeneous state exists).

In order to explain the existence of multiple pseudo stationary homogeneous solutions for the Brusselator model, we make use of Fig. 3 and attempt the following explanation. From this figure can be inferred that in the period  $AB$  the concentration at the centre point almost approaches zero. Since for a long time the concentration profiles

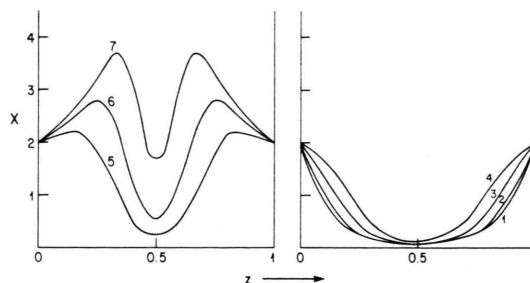


Fig. 4. Propagating fronts for fixed boundary conditions.  $L = 0.6$ ,  $B = 5.4$ ,  $D_A = 0.02$

(a) Profile	1	2	3	4
Time	20.25	21.66	25.56	29.4
(b) Profile	5	6	7	
Time	35.76	36.06	36.25	

remain flat in the central portion of the system, the effect of diffusion here can be neglected.

In this case our equations became

$$dX/dt = A + X^2Y - (B + 1)X \quad (16)$$

and

$$dY/dt = -X^2Y + BX. \quad (17)$$

In order to obtain the homogeneous solutions we set  $dX/dt = dY/dt = 0$  and solve the resulting algebraic equations which are given as

$$A + X^2Y - (B + 1)X = 0 \quad (18)$$

and

$$BX - X^2Y = 0. \quad (19)$$

If  $X \cong 0$ , to satisfy (18),  $A \cong 0$ . If we take a value of  $D_A \cong 0.002$  and  $L = 0.4$ ,  $A$  at the center  $\cong 0.02$ . These  $X \cong 0$  satisfies (18). Now from (19) one can obtain  $X = 0$  and  $X = B/Y$  as the solutions. The root  $X = B/Y$  further shows that since  $B$  is constant, an increase in  $X$  is accompanied by a corresponding decrease in  $Y$  which is observed in the solution of full PDE's for this case. These multiple pseudo-stationary states probably give rise to the propagating fronts which are shown in Figure 4(b). To investigate the effect of diffusion of  $A$  on the relaxation oscillations,  $D_A$  was changed from 0.1 to 0.0002 for zero flux as well as fixed boundary conditions and the observed oscillations have been reported in Figure 5. The dashed lines in this figure show oscillations for zero flux boundary conditions while the solid lines are for fixed boundary conditions. This plot reveals that for the same parameters, the oscillation period for the fixed boundary conditions is

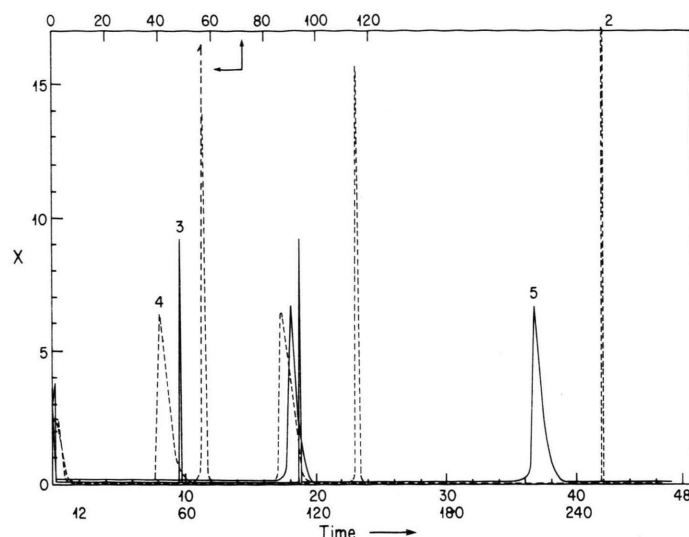


Fig. 5. Oscillations of the centre point.  
 - - - Zero flux boundary conditions;  
 — fixed boundary conditions.

Curve	1	2	3	4	5
$L$	0.4	0.4	1.0	0.6	0.6
$B$	5.4	5.4	5.4	5.4	5.4
$D_A$	0.001	0.0002	0.02	0.02	0.02

almost twice than that for the zero flux boundary conditions. Also, a comparison of curves 1 and 2 indicates that as  $D_A$  decreases, the period of oscillation as well as the amplitude of oscillation goes up. However, in all cases, the nature of the space profiles (standing wave and propagating fronts) remains the same. It was also noticed that for the chosen parameters fixed boundary conditions always resulted in symmetrical structures while for the zero flux boundary conditions asymmetric space profiles are possible. A typical transient profile, for the zero flux boundary conditions, illustrating the development of a propagating front from a standing wave is shown in Figure 6. Another observation made in this study indicates that when  $D_A \rightarrow \infty$ , for the systems of low size all space points fall on the same limit cycle. However, when  $D_A$  assumes low values (say 0.002), two distinct but interwoven limit cycles are observed for the center and the boundary points. If we extrapolate the above mentioned arguments, it can be said that when  $D_A$  assumes very low values, the development of shock structures from seemingly quiescent medium might be observed. As mentioned earlier, a nonuniform distribution of the component  $A$  causes simultaneous propagation of fronts either boundaries towards the center. We have also calculated for a different set of parameters and initial conditions, a different type of relaxation oscillations where the amplitude of oscillations for the center point is quite small (Figure 7). For this case we observed a single propagating front moving from left to the center for a short period (during the

phase  $BA$ ), which is shown in Fig. 8a, while an identical front moves from the right to the center (during the phase  $B'A''$ ) for another short interval (Figure 8b). These fronts however, do not reach the centre but disappear in between. It was also noticed

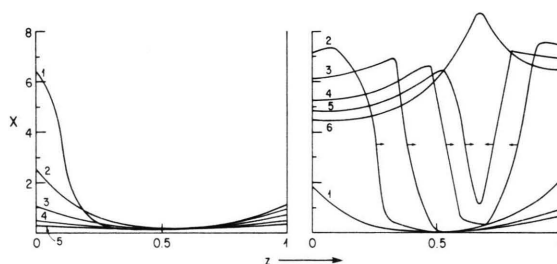


Fig. 6. Propagating fronts for zero flux boundary conditions:  $L = 0.6$ ,  $B = 5.4$ ,  $D_A = 0.02$ .

(a) Profile	1	2	3	4	5	
Time	0.1	4.6	5.82	6.03	6.13	
(b) Profile	1	2	3	4	5	6
Time	7.35	7.62	7.82	8.02	8.07	8.21

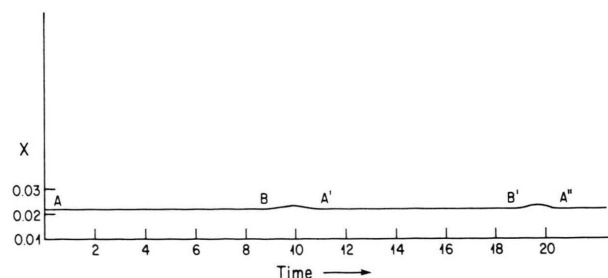


Fig. 7. Oscillations of the centre point.  $A = 1.7$ ,  $B = 4.28$ ,  $L = 1.0$ ,  $D_x = 0.01$ ,  $D_y = 0.0$ ,  $D_A = 0.02$

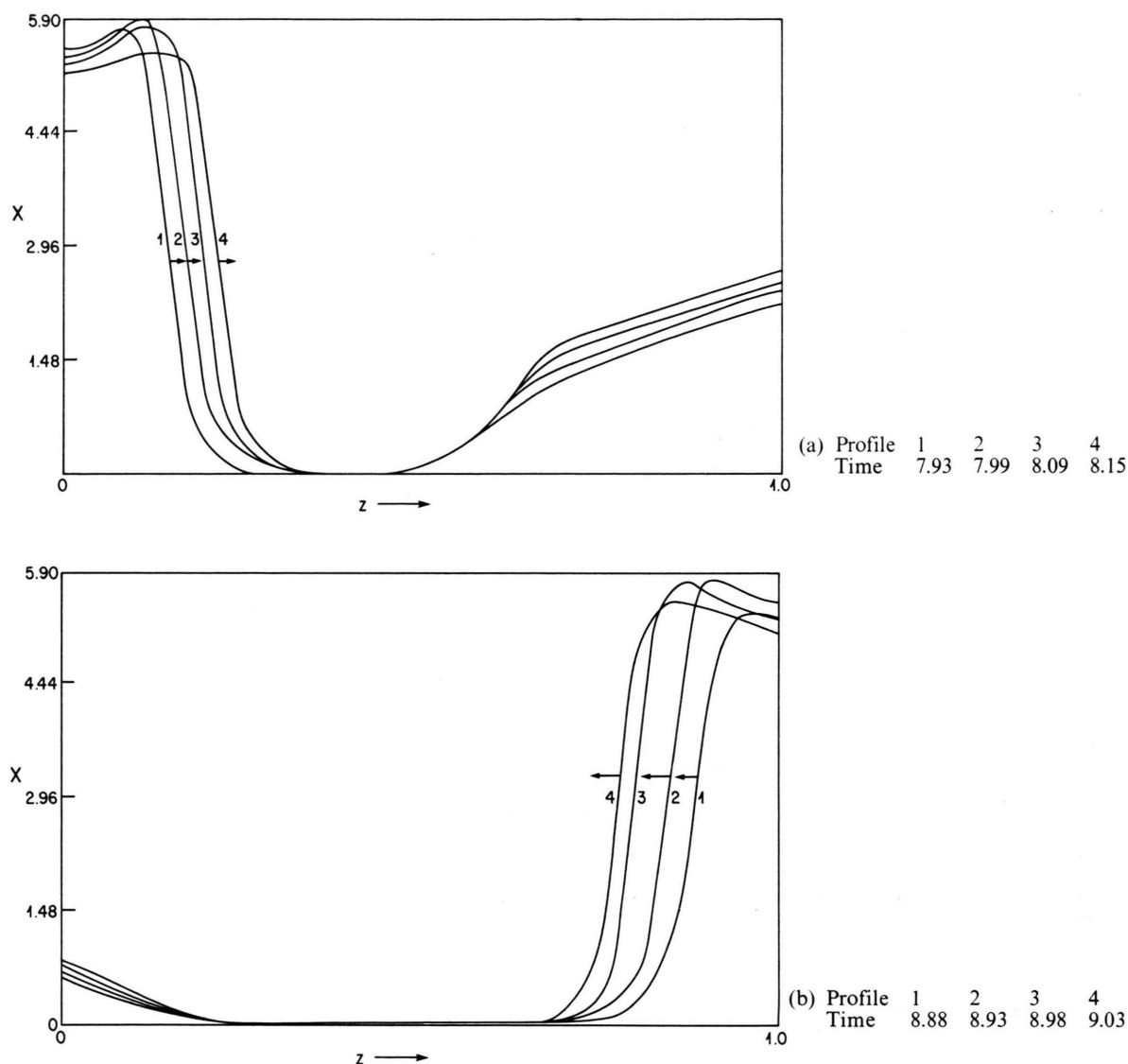


Fig. 8. Single propagating front for zero flux boundary conditions. Parameters same as for Figure 7.

that an increase in the system dimension or a decrease in diffusion coefficients increased the phase difference between various spatial points. As can be expected, a nonuniform distribution of the component  $A$  affects stability and the reported bifurcation analysis of the Brusselator model by Herschkowitz-Kaufman [1] is not applicable here. The bifurcation theory (for  $D_A \rightarrow \infty$ ) predicts a homogeneous stable solution for the parameters

$A = 2.0$ ,  $B = 5.4$ ,  $L = 0.4$ ,  $D_x = 0.008$  and  $D_y = 0.004$  for constant boundary conditions. However, when  $D_A = 0.1$ , the same parameters yield a periodic solution with standing wave characteristics. Our one point collocation approach did show this stability change and the solution of the corresponding ODE's showed oscillations for the center point.

Our numerical experiments for the periodic boundary conditions resulted in a travelling wave

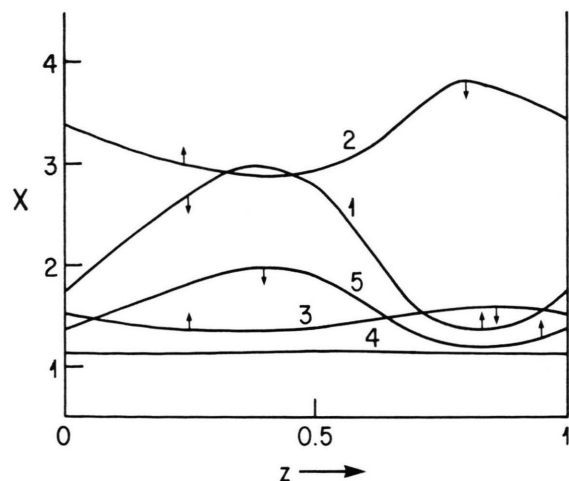


Fig. 9. Two standing wave pattern for periodic boundary conditions.  $A = 2.0$ ,  $B = 5.4$ ,  $D_x = 0.008$ ,  $D_y = 0.004$ ,  $L = 2.0$ .

Profile	1	2	3	4	5
Time	2.74	3.44	4.78	5.58	6.24

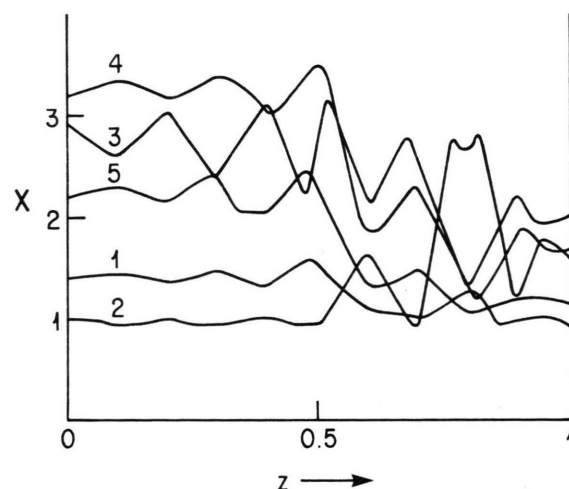


Fig. 10. Incoherent wave pattern for zero flux boundary conditions.  $A = 1.7$ ,  $B = 4.28$ ,  $L = 100$ ,  $D_x = 1.0$ ,  $D_y = 0.0$ .

Profile	1	2	3	4	5
Time	0.1	1.2	2.57	2.82	3.48

and multiplicity of standing waves. Figure 9 illustrates a typical two standing waves pattern. It can be easily observed that each is a nonlinear wave and the two waves are out of phase with each other. The duration for which each wave is observed during a period, however, is not the same. For high values of  $L$  or low diffusion coefficients, we have observed

periodic solutions of increasing complexity. A typical periodic solution is shown in Fig. 10 which describes a multipeak standing wave with incoherent pattern. In general, it has been noticed that multi-peak (high wave number) periodic solutions are possible only at high system lengths. Also the periodic solutions for zero flux or the periodic boundary conditions at high system lengths have similar characteristics.

### c) Dissipative Structures in Two-Dimensions (Rectangular Geometry)

The theory of linear stability analysis indicates that bifurcation from the homogeneous stable solution takes place when at least one eigenvalue of the matrix  $[A - \lambda_n D]$  has a positive real part. The matrix  $A$  for the Brusselator model can be expressed as

$$A \equiv \begin{bmatrix} a_{11} & a_{12} \\ a_{21} & a_{22} \end{bmatrix},$$

where

$$a_{11} = \partial F / \partial X, \quad a_{12} = \partial F / \partial Y,$$

$$a_{21} = \partial G / \partial X, \quad \text{and} \quad a_{22} = \partial G / \partial Y.$$

$F$  and  $G$  are given as

$$F = A + X^2 Y - (B + 1) X \quad \text{and} \quad G = B X - X^2 Y.$$

All the required derivatives are evaluated at  $X_0$ ,  $Y_0$  which is the solution to  $F = 0$ ,  $G = 0$ . The matrix  $D$  is a diagonal matrix of the diffusion coefficients and  $\lambda_n$  are the eigenvalues of the following scalar equation [16].

$$\nabla X + \lambda X = 0 \quad \text{for} \quad X \in \Omega. \quad (20)$$

For the one dimensional model  $\lambda_n$  are given by  $n^2 \pi^2 / L^2$  for both zero flux as well as fixed boundary conditions where

$n = 0, 1, 2, \dots$  for zero flux boundary conditions and  
 $= 1, 2, \dots$  for fixed boundary conditions.

For the two dimensional (rectangular geometry) model  $\lambda_n$  are given by

$$\lambda_n = \pi^2 (m^2 + \delta^2 n^2) / L^2,$$

where  $\delta$  is the aspect ratio (height/length) and  $m$  and  $n$  have the same values as  $n$  for the one dimensional system. From the analysis mentioned above, one clearly observes that when  $\delta = 1$  and  $m = 0$ , the



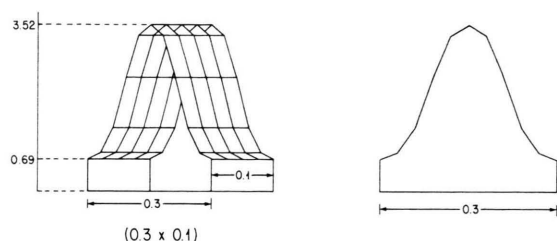


Fig. 11. Two dimensional analogue of one dimensional space structure.  $L = (0.3 \times 0.1)$ .

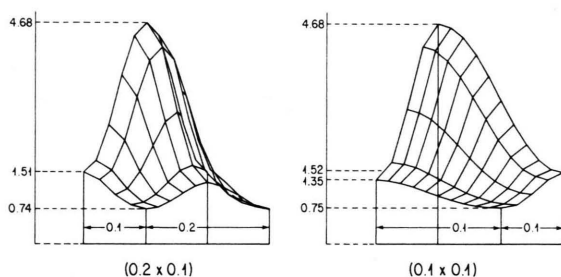


Fig. 12. Symmetric and asymmetric space structures in two dimensions. (a)  $L = (0.2 \times 0.1)$ ; (b)  $L = (0.1 \times 0.1)$ .

bifurcation pattern of one and two dimensional systems is the same. In other words, the parameter values for which the one dimensional system shows bifurcation will also cause bifurcation for the two dimensional case. In our numerical calculations we have, therefore, used the same parameters as those used for the one-dimensional calculations. One can further observe that if in the reaction diffusion equation

$$\frac{\partial X}{\partial t} = F + D_x \left[ \frac{\partial^2 X}{\partial x^2} + \frac{\partial^2 X}{\partial y^2} \right], \quad (21)$$

one of the second derivatives is set to zero, the system will be reduced to the one-dimensional description. In such a case, all one-dimensional steady state solutions will be the solutions in two dimensions with no gradient along  $x$  or  $y$  direction (depending upon whichever second derivative is set to zero). We have tested this observation for the zero flux boundary conditions. For  $L = 0.3$  and  $\delta = 1$ , we have calculated a steady state solution in one dimension and constructed a two dimensional solution starting from it. The calculated steady state solution and the corresponding one dimensional solution are shown in Figure 11. For this case we also calculated some additional steady state solutions in two dimen-

sions by knowing the one dimensional profiles. Variation of the aspect ratio does not affect the qualitative as well as quantitative nature of these solutions as is apparent from the analysis. It should, however, be noticed here that the above mentioned analysis applies only to the case when the component  $A$  is assumed to be constant ( $D_A \rightarrow \infty$ ). When  $A$  is distributed nonuniformly, the resulting steady state solutions are qualitatively similar but quantitatively different. The two dimensional solutions obtained from the one dimensional profiles are termed as 1- $D$  analogues. Apart from these 1- $D$  analogues we have also calculated some other symmetric as well as asymmetric solutions. Some of these are reported in Figure 12. The reported asymmetric solutions are found to be mirror image of one another. Further, by using the symmetry properties, we can obtain 4 steady-states from one solution. Another interesting property observed for the zero

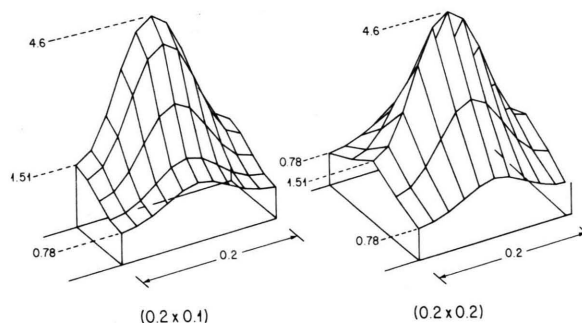


Fig. 13. Composing solutions in two dimensions. (a)  $L = (0.2 \times 0.1)$ ; (b)  $L = (0.2 \times 0.2)$ .

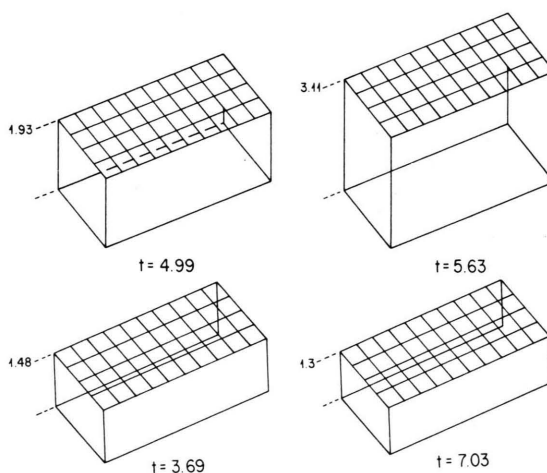


Fig. 14. Two dimensional analogue of homogeneous periodic solution.  $L = (0.2 \times 0.1)$ .

flux boundary conditions was that of composing solutions for systems of high size knowing the steady state solutions for a low size. A typical result is shown in Figure 13. Such composing of solutions in one dimension has already been discussed by Kubicek et al. [6]. As mentioned earlier since all one dimensional solutions are solutions in two dimensions (under certain conditions), we could calculate the analogue of one dimensional periodic solutions

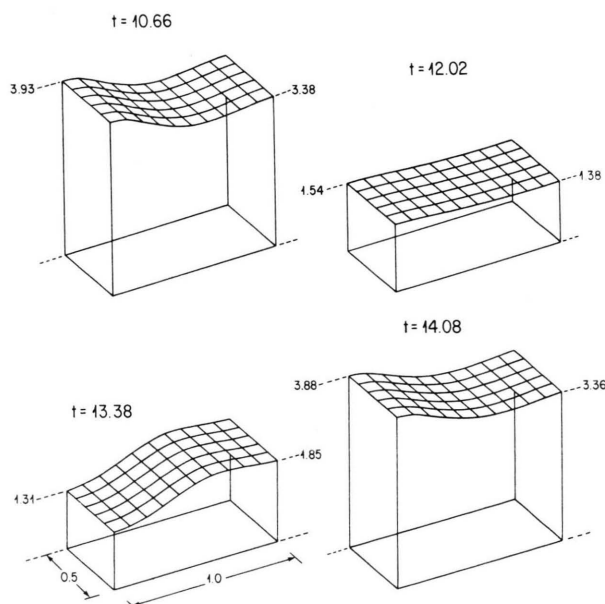


Fig. 15. Two dimensional analogue of a standing wave.  $L = (1.0 \times 0.5)$ .

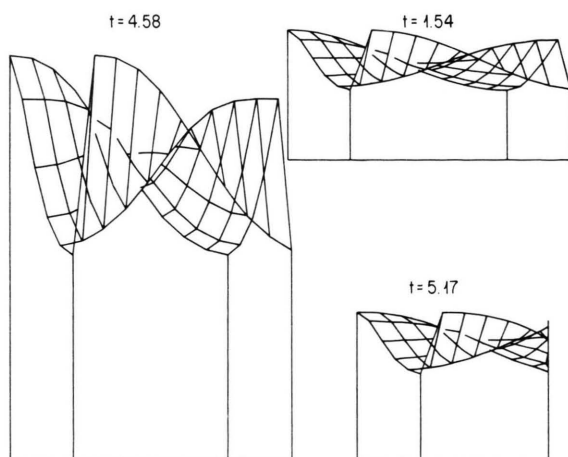


Fig. 16. Antisymmetric periodic structures.  $L = (1.6 \times 1.0)$ .

also in two dimensions. The two dimensional analogue of a homogeneous periodic solution is a plane which goes up and down and is shown in Fig. 14 while the analogue of a standing wave is a vibrating plane which moves up and down (Figure 15). The calculations also showed that the period of oscillation for the one and two dimensional case is the same. Another interesting property observed for the periodic solutions for high values of  $L$  ( $1.6 \times 1.0$ ) and for zero flux boundary conditions was anti-symmetry of the periodic structure about the central plane. Our calculations showed that the structure of the solution in the  $XY$  plane is diametrically opposite to that about the plane  $Y = Y/2$ . In other words, if we bisect the solution at the center (parallel to  $X$  axis) and rotate one part by  $\pi$ , the resulting structure will be exactly equivalent to the remaining portion. A typical periodic solution is shown in Fig. 16 which illustrates this point.

## Conclusions

As noticed earlier all solution profiles obtained by the steady state analysis are not stable and a transient approach is required to calculate the asymptotic properties. It is observed that low amplitude (small deviations from the thermodynamic branch) solutions are not stable for fixed boundary conditions while same wave number multiple solutions with different amplitudes are unstable for zero flux boundary conditions. A non-uniform distribution of the component  $A$  alters the bifurcation pattern and the homogeneous stable solution gives rise to a periodic solution. Also, since diffusion of the component  $A$  does not admit trivial solution for the Brusselator model, the primary bifurcating periodic solution itself is space dependent. It appears that an inclusion of nonuniform  $A$  can result in multiple time scales in the system and relaxation type of oscillations occur. It has been shown that propagating fronts observed in this case probably occur because of multiplicity of the homogeneous solutions. Low diffusion coefficients cause high wave number periodic solutions which are of incoherent pattern. The equivalence of one and two dimensional structures can be explained on the basis of lateral uniformity in either directions. It is also noticed that additional interesting phenomena could be observed as the dimension of the system increases.

- [1] M. Herschkowitz-Kaufman, *Bull. Math. Biol.* **37**, 589 (1975).
- [2] P. Ortoleva and J. Ross, *J. Chem. Phys.* **60**, 5090 (1974).
- [3] G. Nicolas, T. Erneux, and M. Herschkowitz-Kaufman, *Adv. Chem. Phys.* **38**, 263 (1978).
- [4] G. Nicolis and I. Prigogine, *Self Organization in Non-Equilibrium Systems*, John Wiley, New York 1977.
- [5] I. Prigogine and G. Nicolis, *J. Chem. Phys.* **46**, 3542 (1967).
- [6] M. Kubicek, V. Ryzler, and M. Marek, *Biophys. Chem.* **8**, 235 (1978).
- [7] I. Prigogine and R. Lefever, *J. Chem. Phys.* **48**, 1695 (1968).
- [8] V. Hlavacek, R. Janssen, D. Roose, P. Nandapurkar, and P. Van Rompay, Submitted to *Chem. Engng. Communications*.
- [9] D. J. Evans, *Mathematics and Computers in Simulation XXI*, 270 (1979).
- [10] V. Hlavacek, R. Janssen, and P. Van Rompay, *Z. Naturforsch.* **37a**, 39 (1982).
- [11] V. Hlavacek and M. Kubicek, *Chem. Eng. Sci.* **26**, 1737 (1971).
- [12] L. M. Pismen, *Phys. Rev. A* **23**, 334 (1981).
- [13] O. Vafeek, P. Pospisil, and M. Marek, *Scientific Papers of the Prague Institute of Chemical Technology*, K14, 179 (1979).
- [14] M. Herschkowitz-Kaufman and G. Nicolis, *J. Chem. Phys.* **56**, 1890 (1972).
- [15] P. Ortoleva and J. Ross, *J. Chem. Phys.* **63**, 3398 (1975).
- [16] K. J. Brown and J. C. Eilbeck, *Bull. Math. Biol.* **44**, 87 (1982).